中國機械工程學刊第四十卷第六期第 635~645 頁(民國一百零八年)
Journal of the Chinese Society of Mechanical Engineers, Vol.40, No.6, pp 635~645 (2019)

Development of a Knee Exoskeleton with Gear-Linkage Adaptive Mechanism

Shih-Hao Yeh*, Zhi-Hao Kang**, Hsiang-Yuan Ting**
and Han-Pang Huang***

Keywords：Knee exoskeleton, Ergonomics, Vision-based parameter identification.

ABSTRACT

In this paper, we design a novel knee exoskeleton - Gear Linkage Adaptive Knee Joint (GLAKJ), with ergonomic characteristics, i.e., self-rotation and rolling-sliding of the knee joint, which are derived from the bones and the ligaments of the knee joint model, and it is hard to design simultaneously in a simple mechanism. To overcome the difficulties, we construct the GLAKJ which combines the two output motions into a single input mechanism. This ergonomic design can reduce the discomfort causing by the inconsistency between the knee joint and the exoskeleton. On the other hand, we use a vision-based system to measure the knee joint data for parameters identification. The vision-based method requires only a low-cost device to customize the GLAKJ for patients. In the experiments, the measured knee joint data of three subjects are validated and implemented on the proposed exoskeleton, and the results have similar motion like the human knee joint.

INTRODUCTION

Recently, deeper understandings of the human skeletal system and advances in technology have led to increased average lifespans; however, physical deterioration has yet to be overcome. One serious problem is joint deterioration (Daltroy, 1992; Yamada, 2002), which undermines one's ability to walk and run. This is not only inconvenient for one's daily life, but also depriving his dignity. The same holds true for those who suffer from joint disease. It is increasingly important to develop medical techniques (Perry, 2007; Zoss, 2006) to treat joint diseases in the future, such as exoskeletons. For the elderly, exoskeletons can provide extra power to the body (Kong, 2006), enhance mobility and compensate for the lack of energy in completing daily tasks (Pratt, 2004; Shepherd, 2017). For patients, exoskeletons serve as an auxiliary skeletal system for rehabilitation and are indispensable for the paralyzed (Veneman, 2007). Nevertheless, if the design of the exoskeleton is inconsistent with the joint motion, it would be harmful to the wearer.

Paper Received April 2019. Revised June, 2019. Accepted July, 2019. Author for Correspondence: Zhi-Hao Kang.

* *M.S. Student, Department of Mechanical Engineering, University of Washington, Seattle, WA 98195, U.S.*

** *Ph.D. Student, Department of Mechanical Engineering, National Taiwan University, Taipei, Taiwan 10617, ROC.*

*** *Professor, Department of Mechanical Engineering, National Taiwan University, Taipei, Taiwan 10617, ROC.*

The knee joint is one of the most complex and important joints in the human body. It determines the fluency of mobility (Stauffer, 1977) and can cause significant differences in walking patterns. Much research has been focused on developing knee exoskeletons. At first, knee exoskeletons were designed to have a one-degree-of-freedom (DOF) rolling pivot. This design assumed that the biological knee joint had only 1 DOF rolling pivots (Dollar, 2008; Sup, 2008; Wu, 2016). Under this assumption, the design processes for knee exoskeletons were simplified. However, as increasing amount of research had revealed that biological knee joints were not simple rolling pivots (Choi, 2016; Kuan, 2014; Liao, 2015; Ling, 1997; Tucker, 2013; Chaichaowarat, 2017), and this assumption appears to underestimate the motion of the knee joint. Knee-joint motion consists of interactions among the femur, tibia and several ligaments. The convex structure at the end of the femur and the upper part of the tibia forms a sliding interface, and makes it a high degrees of freedom mechanism. A rolling-sliding phase switch during knee motion has also been discussed (Ling, 1997; Wang, 2014). If simplified exoskeleon models are equipped on biological limbs. It would be misalignment (Zanotto, 2015) between the exoskeleton and the limb, leading to uncomfortable wearing experiences.

As more anatomical research about the human knee was conducted, researchers (Huiskes, 1991; J.Wismans, 1980) proposed various exoskeleton designs to compensate or mimic the motion of biological knee joints. One remarkable characteristic about knee motion is the 2-DOF trajectory of a fixed point on the tibia. During flexion and extension, the movement trajectory of a fixed point on the tibia differs from that of a circular pivot (i.e., not a constant radial distance to the knee joint). To remove the above mentioned assumptions regarding the knee's pivot mechanism, some researchers used four-bar linkages (Tucker, 2013; Chaichaowarat, 2017), five-bar linkages (Kuan, 2014; Liao, 2015), cam slots (Wang, 2014), or pulley mechanisms (Choi, 2016) to generate the trajectories that are more complex than the 1-DOF rolling pivot. Most research develops their own exoskeletons with the trajectory of a fixed point on a tibia. However, the knee motion consists of relative motion between the femur and the tibia, in combination with the ligaments, so it is doubtful that the motion of the tibia can be described using a single point. This is related to the rolling-sliding property of knee joints, which is a relatively new concept. If the tibia follows a different rolling pattern compared to the exoskeleton, extra forces and torques would be applied to the ligaments. This may reduce the efficiency of rehabilitation among patients with ligament injuries (Girgis, 1975), possibly causing additional injury.

An ergonomic exoskeleton can reduce the discomfort caused by a mismatch between exoskeleton and limb. To achieve ergonomics, the mechanical design relies on the biological joint measurement methods which can be generally divided into two categories as the intrusive method and the non-intrusive method. The intrusive method (anatomy) can get the physical structure of knee joint but the accuracy for the properties of knee motion is uncertain and involve medical and invasive risks. The non-intrusive data measurement is a popular method for design and analysis, such as vision-based (Pfister, 2014; Kobayashi, 2015), X-ray (Gray, 2017), and MRI methods (Wang, 2014). These methods provide a more practical and efficient way for data collection of biological limb movements. Although X-ray and MRI can acquire information about the interior (bone trajectory), these devices need to be in a special environment and contain radioactive materials. The vision-based methods gather information from the body's exterior. The visual capture devices, e.g., VICON (Kobayashi, 2015) or simple camera, do not harm the human body and provide a certain of data accuracy. Due to the advantages of the resolution and low cost, the vision-based methods has been widely used in the design of exoskeleton in recent years.

In this paper, we derived the mathematical model of human knee joints and designed a two-motion-combined-mechanism knee exoskeleton, called Gear Linkage Adaptive Knee Joint (GLAKJ). The design performs a hybrid motion to mimic the complexity of biological knee joint with simply one input. During the design process, we are dealing with only knee joint motion instead of the whole lower limbs' gait, and we chose the vision-based method to validate the accuracy of the model. Finally, we provides evidence that the proposed design can perform similar movement patterns as the human knee joint.

HUMAN KNEE JOINT MODEL

The knee joint contains four main bones (i.e., the femur, the tibia, the patella, and the fibula) and four ligaments (i.e., the anterior/posterior cruciate ligaments and the medial/lateral collateral ligaments). The bones are driven by muscles and constrained by ligaments. These components constitute the motions of the knee joint as extension/flexion, inner/outer rotation and side rotation. In the design of the knee exoskeleton (Huiskes, 1991), the inner/outer rotation and the side rotation are relatively small compared to the extension/flexion, so the motions are almost negligible in the knee joint modeling.

The two bones (femur and the tibia) at the knee joint are held together by ligaments, as shown in Fig.1. On the contact surfaces of these two bones, the convex structure at the end of the femur has a non-circular contour, and the upper part of the tibia has a platform-like structure.

In Figure 1-(a), a fixed point P_f is defined on the end convex structure of femur and C_i is the initial contact point of tibia and femur. Two markers

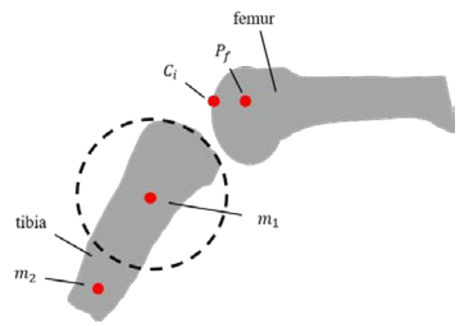

(a)

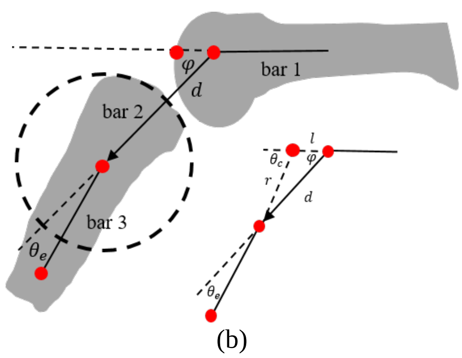

(b)

Fig. 1. (a) Knee joint model (b) Sagittal plane of the knee joint model.

m_1 and m_2 are defined on the tibia. In Fig. 1-(b), bar 1 and bar 3 represent the distance between the femur and the tibia, bar 2 represents the vector from P_f to m_1 and the distance is defined as d. The distance from C_i to m_1 is r.

In the previous study (Stauffer, 1977), the contour of the platform structure of the tibia is assumed as a portion of a circular arc, instead of an ellipse, with radius equal to the distance from m_1 to the knee joint contact surface. However, the motions of the knee joint is not only rolling but also sliding on the surface of the femur's convex end during the knee flexion. The femur and the tibia are connected with ligaments and muscles so that the motions of knee joint is not simply a rolling pivot with a fixed center of rotation. In other words, d is not a constant distance. Moreover, bar 2 and bar 3 (Fig.1-(b)) are not parallel during the extension/flexion motions.

To derive the rolling-sliding characteristics of the knee joint model, two angles needs to be defined. The angle φ is defined as the knee-rotation between bar 1 and bar 2 (the horizontal line). The self-rotation angle θ_e is defined as the angular variation caused by the rolling-sliding effect, i.e., the angle between bar 2 and bar 3. After introducing the motion of the knee joint and the model parameters, we can derive a function for rolling-sliding characteristics as

$$d(\varphi)=\frac{2l\cos\varphi\sqrt{(2l\cos\varphi)^2-4(l^2-r^2)}}{2} \qquad (1)$$

$$r^2=l^2+d^2-2ld\cos\varphi \qquad (2)$$

where $d(\varphi)$ is a change of radial distance. When the knee rotates, the rotation angle φ is directly related to r which is a function of θ_c, and θ_c is a function of φ. The relationship between φ and r define a change of radial distance from m_1 to P_f instead of a constant radial distance. In addition, the self-rotation angle θ_e can be derived as

$$\theta_e=\cos^{-1}\frac{V_{Pm1}\cdot V_{m12}}{\|V_{Pm1}\|\|V_{m12}\|} \qquad (3)$$

where V_{Pm1} and V_{m12} are the vector from P_f to m_1 and the vector from m_1 to m_2, respectively. In this section, we discussed the human knee joint model. In order to achieve the ergonomics, the exoskeleton design is based on the human joint knee model with rolling-sliding characteristics. The following will introduce the mechanical design of the GLAKJ.

MECHANICAL DESIGN OF THE GLAKJ

The novelty knee joint exoskeleton GLAKJ is designed as a gear linkage mechanism. It combines the two motion types, i.e., rolling and sliding, into a single-input mechanism. In the previous study (Wang, 2014), the authors had been verified that the passive rotary pin (to reduce the misalignment between femur and tibia) can reduce the internal forces and torques acting on the interface of limbs and exoskeletons to achieve ergonomics. In this paper, the GLAKJ provides a more robust mechanism. The passive rotary pin is replaced by an active rotary, and it can be adapted to different people by adjusting the gears to achieve the ergonomic exoskeleton. The mechanism of the GLAKJ is shown in Fig. 2.

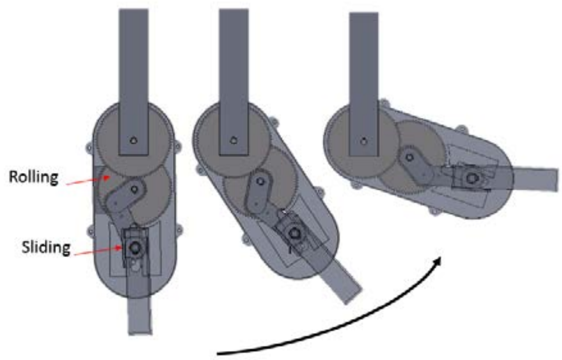

Fig. 2. The gear linkage adaptive knee joint.

The transmission components of the GLAKJ are composed of a gear train (eight gears) and a linear slot, as shown in Fig.3. The circles marked with g indicates the gear, and the subscript is the number of the gear. The reduction ratio between g_3 and g_4 is caused by the transduction of four gears. The two rectangles represent the connectors for wearing on

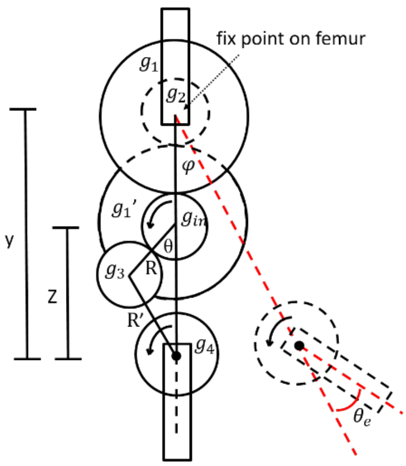

Fig. 3. The gear train mechanism of the GLAKJ

the upper and the lower legs. The gears g_1 and g_2 are fixed on the upper connector, in which the center point is analogous to point P_f in the knee joint model, and g_4 is fixed on the lower connector. g_{in} is the input gear and the shaft of g_3 is fixed on g'_1. The distance between the center point of g_3 and g_{in} is defined as R. The distance between the center point of g_3 and g_4 is R', and the distance between the center point of g_{in} and g_4 is Z.

The movement of the GLAKJ can be illustrated in details by Fig. 3. Given an input motion g_{in}, the whole mechanism is rotating about g_1 and g_2 with angle φ. Meanwhile, g'_1 is passively driven. Since the shaft of g_3 is fixed on g'_1, the angle θ is decreasing. Also, the shaft of g_4 is constrained to the linear slot so that g_4 is pushed toward the radial direction. This 2-DOF trajectory belongs to the trajectory of the center point of g_4 corresponding to the knee-rotation angle φ.

Since different values of φ correspond to different values of θ, the length of Z is changed by the initial angle of θ and the length of R and R'. On the other hand, g_4 is linked with g_{in} through a series of gears so the rotation of g_{in} drives g_4 to rotate θ_e. Therefore, the radial displacement of the center point of g_4 and the rotation θ_e are combined and function simultaneously.

MATHEMATICAL MODELS OF THE GLAKJ

To realize the knee exoskeleton, the following will introduce the mathematical models of the GLAKJ for parameter identification. The algorithms include the rolling-sliding functions, tibia trajectory and the Slide/Roll ratio. The rolling-sliding functions are used to define the relationship of the gear chain. Tibia trajectory is used to calculate the measured trajectory from the vision sensors. The Slide/Roll ratio defines the characteristics from the different rotation angles of the knee joint.

Rolling-sliding functions of the GLAKJ

The rotation and displacement of the knee joint are constructed by the gear chain. In order to formulate the kinematics of the GLAKJ, we first derive the function of rotation. From the input gear g_{in} to the output gear g_4, the relation of the four gears (g_1, g'_1, g_2, g_{in}) can be formulated as

$$\theta_{in} r_{in} = r_1 \varphi \tag{4}$$

$$\varphi r_2 = r'_1 \theta'_1 \tag{5}$$

$$\theta = \theta_{initial} - \theta'_1 \tag{6}$$

where r and θ represent the radius of the gear and rotation angle, respectively. Subscript represents the number of the gear. $\theta_{initial}$ is the initial angle of θ. The functions of the rotation angle φ and θ are

$$\varphi = \frac{r_{in}}{r_1}\theta_{in} = \frac{r'_1}{r_2}\theta'_1 \tag{7}$$

$$\theta = \theta_{initial} - \frac{r_2}{r_1}\varphi \tag{8}$$

Substituting (7) into (8), θ can be derived as

$$\theta = \theta_{initial} - \frac{r_{in} r_2}{r_1 r'_1}\theta_{in} \tag{9}$$

On the other hand, the self-rotation angle θ_e is only related to g_{in} and g_4 as the gear-pair relation

$$\theta_{in} r_{in} = r_3\theta_3 = r_x\theta_x = r_4\theta_4 \tag{10}$$

Therefore, θ_e can be derived from (10) as

$$\theta_e = \frac{r_{in}}{r_4}\theta_{in} \tag{11}$$

In the displacement of the GLAKJ, the 2-DOF trajectory is mainly caused by the radial displacement y (Fig. 3) which can be derived as

$$y = r_1 + r_2 + Z \tag{12}$$

where r_1 and r_2 are the constant radii of g_1 and g_2, respectively. On the other hand, Z is one of the variable sides of the triangle RZR'. It will change length with θ, and the function of Z is as follows

$$Z^2 + R^2 - 2Z\cos\theta = R'^2 \tag{13}$$

$$Z = \frac{2R\cos\theta + \sqrt{(2R\cos\theta)^2 - 4(R^2 - R'^2)}}{2} \tag{14}$$

The displacement y can be transformed into a function $y(\varphi)$ by substituting (7), (9) and (14) into (12).

According to those functions, the GLAKJ has two angles (φ, θ_e) and a displacement $y(\varphi)$. This mechanism can be driven by a single-input θ_{in} to generate rolling-sliding output as the knee joint motion.

Tibia trajectory of the GLAKJ

The coordinate systems on the GLAKJ correspond to the femur and the tibia. The coordinate **systems** can be used to calculate the trajectory of the calf swing experiments. The measured trajectories are used to determine the gear train specifications as the customized exoskeleton for the patient. To obtain the trajectory on the tibia, the homogeneous transformation matrix is defined as

$$\begin{bmatrix} \cos\theta & \text{-}\sin\theta & 0 & x \\ \sin\theta & \cos\theta & 0 & y \\ 0 & 0 & 1 & z \\ 0 & 0 & 0 & 1 \end{bmatrix} \tag{15}$$

Four coordinates are shown in Fig.4. The frame 0 and the frame 1 are located on the femur, and the former is fixed at P_f. The frame 2 and the frame 3 are analogous to the lower two markers affixed to the calf (tibia).

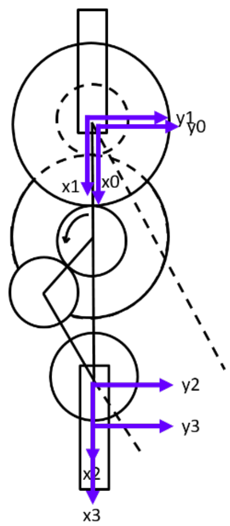

Fig. 4. Four coordinate systems of the GLAKJ.

From frame 0 to frame 3, the transformation matrices are derived as

$$T_1^0 = \begin{bmatrix} \cos\varphi & -\sin\varphi & 0 & 0 \\ \sin\varphi & \cos\varphi & 0 & 0 \\ 0 & 0 & 1 & 0 \\ 0 & 0 & 0 & 1 \end{bmatrix} \tag{16}$$

$$T_2^1 = \begin{bmatrix} \cos\theta_e & -\sin\theta_e & 0 & y \\ \sin\theta_e & \cos\theta_e & 0 & 0 \\ 0 & 0 & 1 & 0 \\ 0 & 0 & 0 & 1 \end{bmatrix} \tag{17}$$

$$T_3^2 = \begin{bmatrix} 1 & 0 & 0 & \overline{m_1 m_2} \\ 0 & 1 & 0 & 0 \\ 0 & 0 & 1 & 0 \\ 0 & 0 & 0 & 1 \end{bmatrix} \tag{18}$$

In order to observe the trajectory of the calf to identify the corresponding tibia, two points m_1 and m_2 at the tibia are derived as

$$m_1 = T_0^1 T_1^2 P_f \tag{19}$$

$$m_2 = T_1^0 T_2^1 T_3^2 P_f \tag{20}$$

where m_1 and m_2 can be measured by the vision sensors . This measured trajectory is used to adjust the appropriate specifications of the gears and compares the trajectory with the GLAKJ as a customized exoskeleton.

Slide/Roll ratio of the GLAKJ

The Slide/Roll ratio (Ling, 1997) is the proportion of sliding motion and rolling motion in knee joints. When the flexion angle of knee joint is over 70 degrees, the motion of knee joint is changed from rolling-sliding to almost only sliding. This indicates that the extension/flexion motions of the knee joint have two phases. Under 60 degrees of flexion, the Slide/Roll ratio is small (about 0~0.5). Over the 70 degrees, the ratio increases dramatically. This characteristic means that the sliding dominates rolling.

When the traveled distance during the whole knee flexion movement has been calculated, the length of the m_1 trajectory over a short period is L multiplied by $d\varphi$. Then, the Slide/Roll ratio is calculated on the contact surface. L can be further multiplied by λ to ensure the trajectory and the end convex of the femur are at scale. The scaled length L' is derived as

$$L' = \lambda L = \lambda y d\varphi \tag{21}$$

$$\lambda = \frac{1}{y_{initial}} \tag{22}$$

where λ is the scaling factor. l is the distance between P_f and C_i. $y_{initial}$ is the initial distance between P_f and m_1. Fig.5 shows the parameter settings on the sagittal view of the knee joint.

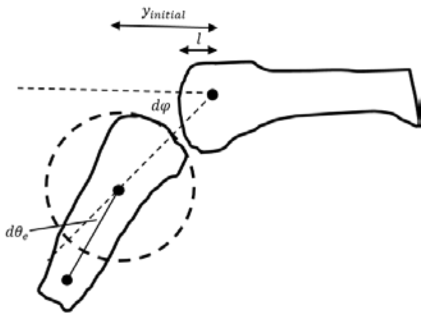

Fig. 5. An illustration of the calculation for Slide to Roll ratio.

The trajectory L includes the rolling-sliding motion. To derive the displacement caused by rolling, a circle is defined with m_1 as its center and the distance between m_1 to the convex end of the femur as its radius. The displacement of the circle rolling with angle $d\theta_e$ is derived as

$$\text{Roll} = (y_{initial} - l)d\theta_e \tag{23}$$

$$\text{Slide} = L' \tag{24}$$

Substituting (21) into (24), the Slide/Roll ratio can be derived as

$$\frac{\text{Slide}}{\text{Roll}} = \frac{\lambda y d\varphi}{(y_{initial} - l)d\theta_e} \tag{25}$$

By combining (7) and (11), $d\theta_e$ can be changed into a function of φ as

$$d\theta_e = \frac{r_1}{r_4} d\varphi \tag{26}$$

Therefore, the Slide/Roll ratio in (25) can be rewritten as

$$\frac{\text{Slide}}{\text{Roll}} = \frac{\lambda y r_4}{(y_{initial} - l)r_1} \tag{27}$$

Since y is a function of φ, the ratio is a function of φ.

PARAMETER IDENTIFICATION

The parameter identification aims to evaluate a consecutive design process from obtaining qualified knee joint data to realizing the GLAKJ. An efficient way to design a well-fitted exoskeleton is to get the knee joint data from the patients and fine-tune the exoskeleton's parameters. In order to obtain the parameters of the GLAKJ, the design process is divided into two parts, as shown in Fig. 6.

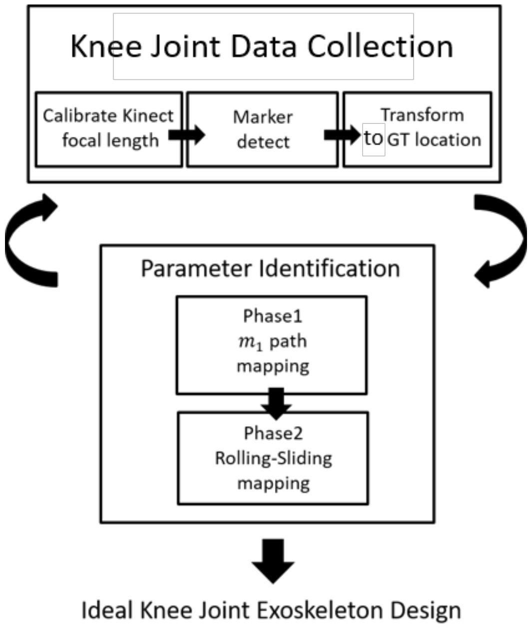

Fig. 6. The proposed design process for an ideal knee joint exoskeleton.

The knee joint data collection uses a vision-based method to measure the trajectory of the calf. The parameters of the GLAKJ are identified by the m_1 path mapping and the rolling-sliding pattern mapping. After the trajectory mapping, the GLAKJ is validated with the measured data to realize the ideal knee joint exoskeleton.

Knee joint data collection

In the knee joint data collection, we use the Microsoft Kinect™ V2 to measure the motion, which is a somatosensory device and can be easily obtained by the average consumer. Four markers are affixed to the lower limb, i.e., two on the thigh and two on the calf, as shown in Fig.7. The distance between the two markers (thigh or calf) is 10 cm. The middle two

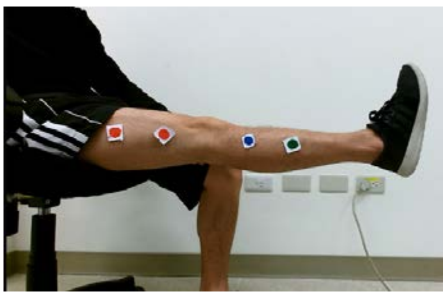

Fig. 7. Four markers on the thigh and the calf for data collection.

markers are placed at 10 cm from the knee joint. Since the femur and the tibia are shaft-like and rigid bodies, the four points are assumed to be enough for representing their motion.

Three subjects participate the parameter identification experiments, including two males and one female. Each subject flexes their knees from 0 to 90 degrees without moving their thighs ($\varphi+\theta_e=90^\circ$). The Kinect camera captures the trajectories of the four markers on the sagittal plane. Since Kinect provides pixel's depth information, the depth value of each pixel needs to translate pixel information into the ground-truth location, as shown in Fig. 8.

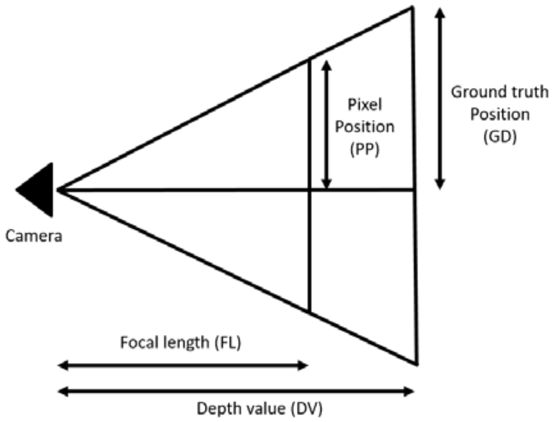

Fig. 8. Translation from pixel position to ground truth position.

The trajectories have been offset toward the *x* or *y* directions and the value of the coordinates is referred to the spatial relative position as follows

$$\text{Ground Truth Position (GD)} = PP\frac{DV}{FL} \qquad (28)$$

where *PP* is the pixel position. *DV* and *FL* are depth value and focal length, respectively. GD represents ground truth position.

Parameter identification

To realize the GLAKJ, several parameters need to be determined, including the radius $(g_1, g'_1, g_2, g_3, g_4, g_{in}, r_1, r'_1, r_2, r_3, r_4, r_{in})$, the center distance (R, R') and the gear reduction ratio r_3/r_4 between g_3 and g_4. The design process is separated into two parts as the 2-DOF trajectory generation and self-rotation of the tibia. They correspond to the m_1 trajectory mapping and rolling-sliding trajectory mapping, respectively.

In the m_1 trajectory mapping, the trajectory of the center point of g_4 is mainly affected by $(r_1, r_2, R, R', \theta)$. First, we fine-tuned the parameters to match the measured m_1 trajectory, and then adjusted the gear reduction ratio r_3/r_4. Adjusting the reduction ratio corresponds to different extra rotatory magnitude of θ_e and affects adherence of the exoskeleton to the biological rolling-sliding effect.

Table 1. Parameters of the GLAKJ

Parameter	Value
r_1 (mm)	38
r_2 (mm)	12
R (mm)	24
R' (mm)	50
$\theta_{initial}$	50°

The parameters are mainly decided through trial and error subject to two considerations: (1) $\theta_{initial}$ cannot be too large because when the length of Z is too small, the shaft of g_4 will collide with the shaft of g_2; (2) at the initial position, the distance between the shafts of g_1 and g_4 needs to be equal to $\overline{P_f m_1}$ to satisfy the model settings. In addition, g_1 and g_2 are configured the same as g'_1 and g_{in}, and all the gear's module is set to 1. The identified parameters are listed in Table 1 and the results of m_1 trajectory mapping are shown in Fig. 9.

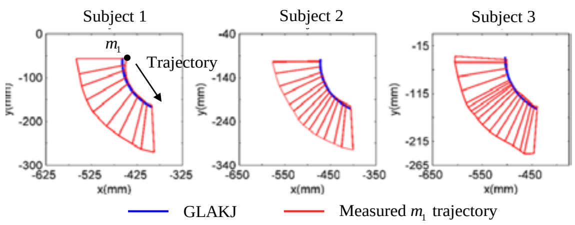

Fig. 9. m_1 trajectory of the GLAKJ (blue) and the measured m_1 trajectory (red).

The second experiment is the rolling-sliding trajectory mapping. The trajectory-related parameters are fixed and then the r_3/r_4 ratios are fine-tuned. In the experiments, three r_3/r_4 ratios are chosen to compare the trajectory of the GLAKJ with the measured data. The r_3/r_4 ratios are chosen as 0, 5/10 and 5/40, and $r_3/r_4=0$ means the self-rotating θ_e is eliminated.

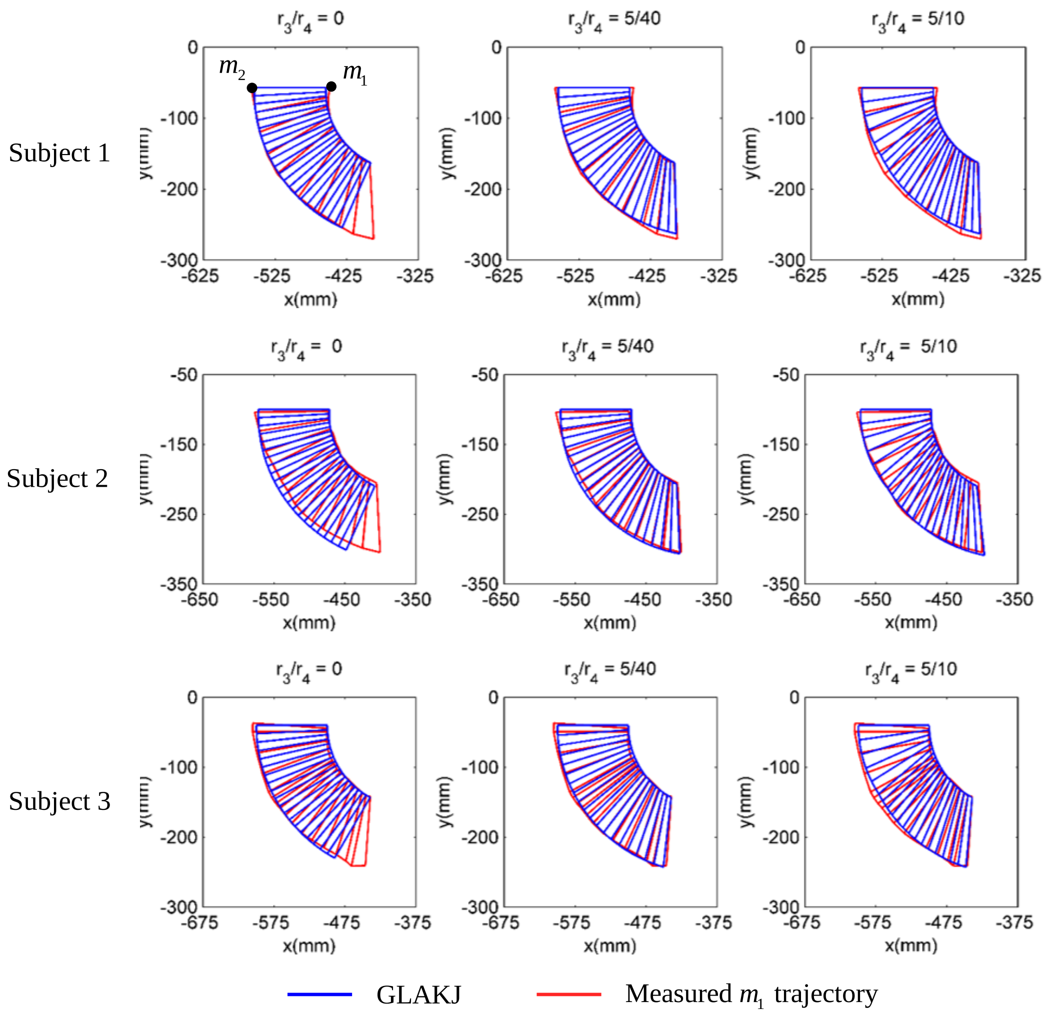

Fig. 10. The rolling-sliding trajectories of the GLAKJ (blue) compare with the measured trajectory (red). Rows-Subjects and Columns- r_3/r_4 ratio .

The experimental results of three subjects are shown in Fig.10. The results of $r_3/r_4=0$ and $r_3/r_4=5/10$ show that although m_1 trajectories are matched, the trajectories of the GLAKJ (Fig.10-blue) mismatch the entire calf trajectories (Fig.10-red). When $r_3/r_4=0$, the exoskeleton tends to roll slower than the biological knee joint, whereas, $r_3/r_4=5/10$ is a faster-rolling. When $r_3/r_4=5/40$, the self-rotation angle increases at a relatively slow pace, and there is a strong match bet the exoskeleton and physical data. Therefore, we choose this ratio for the exoskeleton realization.

EXPERIMENTS

A prototype of the GLAKJ is implemented by the 3D printer, as shown in Fig. 11. The NI myRIO platform is used as a controller. Since the proposed exoskeleton design aims to simplify the control complexity of a high-DOF mechanism, the GLAKJ only uses one servo as an input to generate the 2-DOF movement. Two rotary potentiometers are used to measure the angle displacements of φ and θ_e, and one linear potentiometer is used to measure the linear displacement of the g_4 shaft's dy. dy and θ_e are plotted as function of φ. Since the calf connector rotation is measured up to 90 degrees $(\varphi+\theta_e)$, φ is only 60 degrees.

The 3D printed GLAKJ and simulation comparison (Fig.12-(a)) achieves that the GLAKJ has the characteristics of rolling-sliding, and the result is similar to the simulation. This low-cost exoskeleton has two movements in the knee joint. On the other hand, the results of the self-rotation (Fig.12-(b)) is not as good as the results of rolling-sliding. The maximum deviation angle is about 3 degrees. The reason is that the 3D printed gear is not accurate (backlash) and low resolution sensors result in partial disturbances. Overall, the feasibility of the design is validated.

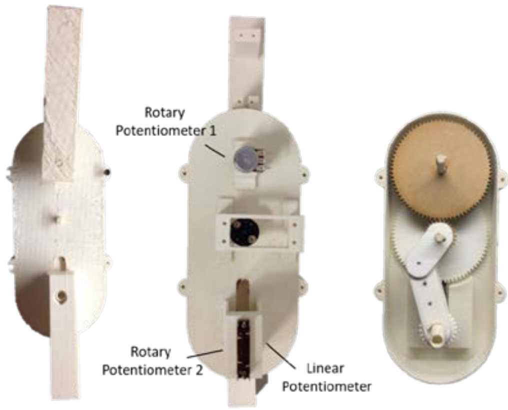

Fig. 11. The 3D-printed mechanism of the GLAKJ.

On the other hand, the Slide/Roll ratio of the GLAKJ can satisfy the proportion of sliding and rolling motion in knee joints by the mechanism of a blocking wall and a torsion spring, as shown in Fig. 13-(a).

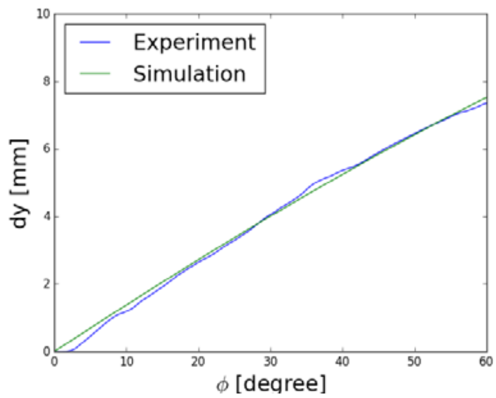

(a)

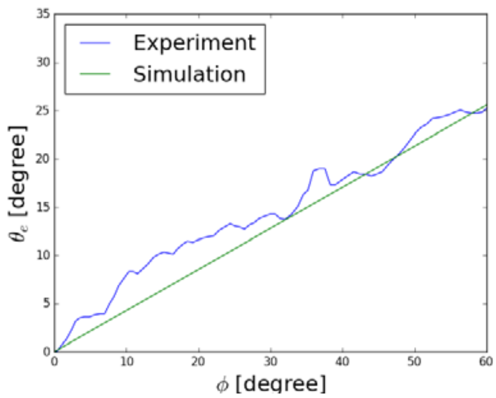

(b)

Fig. 12. The experiments and simulations result of (a) (dy,φ) and (b) (θ_e,φ).

In Fig. 13-(a), the switching angle of rolling-to-sliding is defined as θ_{thres} which is the limitation of θ_e. This clutch mechanism divides the motion into two parts. A torsion spring is placed on the shaft of g_4 and a blocking wall is added to the shield. When $\theta_e = \theta_{thres}$, the blocking wall constrains the motion of the calf connector, i.e., θ_e is fixed. The torsional spring is used to consume the extra rotation caused by g_4.

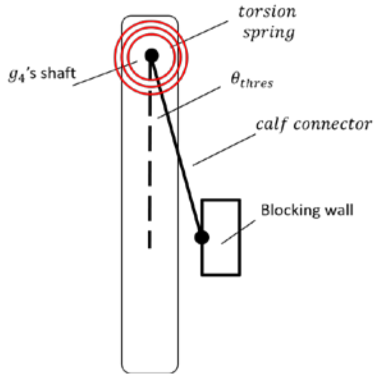

(a)

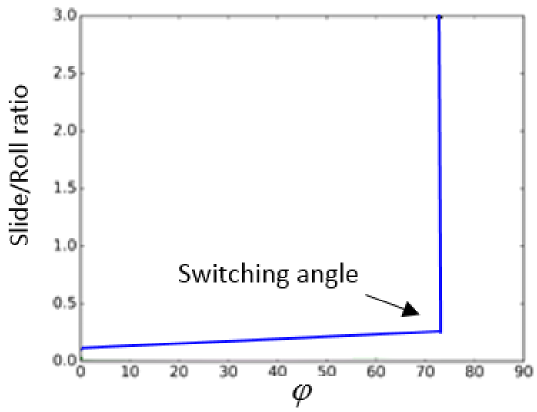

(b)

Fig. 13. (a) The clutch mechanism for θ_{thres}. (b) The Slide/Roll ratio with respect to φ.

The switching angle of the knee joint needs to be obtained from the bone information. However, the vision-based system cannot measure such precise switching process. In order to achieve the ergonomic design, we refer to the bone trajectory in (Ling, 1997) and set $\theta_{thres} = 30^\circ$. The result (Fig.-13(b)) shows that when φ is between 0 and 70 degrees, and the Slide/Roll ratio is slowly increased from 0.1 to 0.3. It means that the GLAKJ is mainly rolling motion in this interval. After the switching angle ($\varphi = 74^\circ$), the ratio increases immediately and decreases the rolling to 0. In the experiments, we used a simple clutch mechanism to constrain the rotation to satisfy the characteristics of the knee joint motion.

CONCLUSIONS

In this paper, we design a novelty knee exoskeleton (GLAKJ) based on the knee joint model, and use the vision-based system to collect the reliable data for parameter identification. We use a low-cost solution to achieve the knee exoskeleton, which only requires single input to satisfy the knee's rolling-sliding motion and the Slide/Roll ratio (over 70 degrees). Finally, the GLAKJ is realized by 3D printer and verified in the experiments. In the future, we will implement the entire lower limb exoskeleton (hip, knee and ankle) and use a more precise vision system, e.g., VICON, to adjust the customized mechanism for patients.

REFERENCES

Chaichaowarat, R., Granados, D. F. P., et al. "Passive knee exoskeleton using torsion spring for cycling assistance," IEEE/RSJ International Conference on Intelligent Robots and Systems, Vancouver, Canada, (2017).

Choi, B., Lee, Y., et al. "A self-aligning knee joint for walking assistance devices," IEEE International Conference of the Engineering in Medicine and Biology Society, FL, USA, (2016).

Daltroy, L. H., Logigian, M., et al. "Does musculoskeletal function deteriorate in a predictable sequence in the elderly?" Official journal of the american college of rheumatology, 5(3), pp. 146-150 (1992).

Dollar, A. M. and Herr, H. "Design of a quasi-passive knee exoskeleton to assist running," IEEE/RSJ International Conference on Intelligent Robots and Systems, Nice, France, (2008).

Girgis, F. G., Marshall, J. L., et al. "The cruciate ligaments of the knee joint. Anatomical, functional and experimental analysis." Clinical orthopaedics and related research, 106), pp. 216-231 (1975).

Gray, H. A., Guan, S., et al. "Accuracy of mobile biplane X-ray imaging in measuring 6-degree-of-freedom patellofemoral kinematics during overground gait." Journal of biomechanics, 57(pp. 152-156 (2017).

Huiskes, R., Blankevoort, L., et al. "The envelope of passive knee joint motion." Journal Biomechanics, 21(9), pp. 705-720 (1991).

J.Wismans, F.Veldpaus, et al. "A three dimensional mathematical model of the knee joint." Journal of biomechanics, 13(8), pp. 677-685 (1980).

Kobayashi, T., Singer, M. L., et al. "The effect of changing plantarflexion resistive moment of an articulated ankle–foot orthosis on ankle and knee joint angles and moments while walking in patients post stroke." Clinical Biomechanics, 30(8), pp. 775-780 (2015).

Kong, K. and Jeon, D. "Design and control of an exoskeleton for the elderly and patients." IEEE/ASME transactions on mechatronics, 11(4), pp. 428-432 (2006).

Kuan, J.-Y., Pasch, K. A., et al. "Design of a knee joint mechanism that adapts to individual physiology," Annual International Conference of the IEEE Engineering in Medicine and Biology Society, Chicago, USA, (2014).

Liao, Y., Zhou, Z., et al. "BioKEX: A bionic knee exoskeleton with proxy-based sliding mode control," IEEE International Conference on Industrial Technology, Seville, Spain, (2015).

Ling, Z.-K., Guo, H.-Q., et al. "Analytical study on the kinematic and dynamic behaviors of a knee joint." Medical Engineering and Physics, 19(1), pp. 29-36 (1997).

Perry, J. C., Rosen, J., et al. "Upper-limb powered exoskeleton design." IEEE/ASME transactions on mechatronics, 12(4), pp. 408-417 (2007).

Pfister, A., West, A. M., et al. "Comparative abilities of Microsoft Kinect and Vicon 3D motion capture for gait analysis." Journal of medical engineering & technology, 38(5), pp. 274-280 (2014).

Pratt, J. E., Krupp, B. T., et al. "The RoboKnee: an exoskeleton for enhancing strength and endurance during walking," IEEE International Conference on Robotics and Automation, LA, USA, (2004).

Shepherd, M. K. and Rouse, E. J. "Design and validation of a torque-controllable knee exoskeleton for sit-to-stand assistance." IEEE/ASME transactions on mechatronics, 22(4), pp. 1695-1704 (2017).

Stauffer, R. N., Chao, E., et al. "Biomechanical gait analysis of the diseased knee joint." Clinical orthopaedics and related research, 126), pp. 246-255 (1977).

Sup, F., Bohara, A., et al. "Design and control of a powered transfemoral prosthesis." The International journal of robotics research, 27(2), pp. 263-273 (2008).

Tucker, M. R., Moser, A., et al. "Design of a wearable perturbator for human knee impedance estimation during gait," IEEE International Conference on Rehabilitation Robotics, WA, USA, (2013).

Veneman, J. F., Kruidhof, R., et al. "Design and evaluation of the LOPES exoskeleton robot for interactive gait rehabilitation." IEEE Transactions on Neural Systems and

Rehabilitation Engineering, 15(3), pp. 379-386 (2007).
Wang, D., Lee, K.-M., et al. "Adaptive knee joint exoskeleton based on biological geometries." IEEE/ASME transactions on mechatronics, 19(4), pp. 1268-1278 (2014).
Wu, J., Gao, J., et al. "The Design and Control of a 3-DOF Lower Limb Rehabilitation Robot." Mechatronics, 33(pp. 13-22 (2016).
Yamada, K., Healey, R., et al. "Subchondral bone of the human knee joint in aging and osteoarthritis." Osteoarthritis and cartilage, 10(5), pp. 360-369 (2002).
Zanotto, D., Akiyama, Y., et al. "Knee joint misalignment in exoskeletons for the lower extremities: Effects on user's gait." IEEE Transactions on Robotics, 31(4), pp. 978-987 (2015).
Zoss, A. B., Kazerooni, H., et al. "Biomechanical design of the Berkeley lower extremity exoskeleton (BLEEX)." IEEE/ASME transactions on mechatronics, 11(2), pp. 128-138 (2006).

NOMENCLATURE

P_f a fixed point on the femur

C_i initial contact point of tibia and femur

m_i points on the tibia

d the distance from P_f to m_1

r the distance from C_i to m_1

ψ knee rotation angle
θ_e self-rotation angle

θ_{thres} switching angle of rolling-to-sliding

V_{Pm} the vector from P_f to m_i

g_i the *i*-th gear

r_i radius of the *i*-th gear

θ_i rotation angle of the i-th gear

R the distance between the center point of g_3 and g_{in}

R' the distance between the center point g_3 and g_4

Z the distance between the center point g_{in} and g_z

Y the radial displacement

T transformation matrix

λ scaling factor

l distance between P_f and C_i

y_{initial} the initial distance between P_f and m_1

L the length of the m_1 trajectory over a period

L' the scaled trajectory

PP pixel position

DV depth value

FL focal value

GD ground truth position

齒輪-連桿自適應機構的膝關節外骨骼開發

葉士豪　　康志豪　　丁相元　　黃漢邦
國立臺灣大學機械工程學系

摘 要

在本文中，我們設計了一個新穎的膝蓋外骨骼-齒輪連桿適應性膝關節。這個外骨骼具有人體工學的特性: 膝關節的自轉以及滾動-滑動，這些特性由膝關節的骨骼與韌帶所產生，且難以同時實現在一個簡單的機構中。為了克服這些難題，我們所設計的外骨骼(GLAKJ)具備單輸入-雙輸出的機構來滿足人體工學的需求，這樣的設計可減少膝關節與外骨骼的運動不一致所產生的不適感。另一方面，我們利用影像基底系統來擷取膝關節的資料進行系統識別，此方法僅需要低成本的裝置即可為病人客製化 GLAKJ。在實驗中，三個受測者的膝關節數據被用來驗證並實現外骨骼機構，實驗的結果顯示，我們所設計的 GLAKJ 可近似於人的膝關節運動。